THE ANATOLIAN JOURNAL OF CARDIOLOGY

Official journal of the TURKISH SOCIETY OF CARDIOLOGY

MiRNA-615-3p Alleviates Oxidative Stress Injury of Human Cardiomyocytes Via PI3K/Akt Signaling by Targeting MEF2A

ORIGINAL INVESTIGATION

ABSTRACT

Background: Myocardial infarction, a coronary heart disease, is a serious hazard to human health. Cardiomyocyte oxidative stress and apoptosis have been considered as the main causes of myocardial infarction. Here, we aimed to investigate the role of miR-615-3p in oxidative stress and apoptosis of human cardiomyocytes.

Methods: Reverse transcription-quantitative polymerase chain reaction was performed to determine miR-615-3p or MEF2A expression in human cardiomyocytes. Apoptosis and viability of human cardiomyocytes were assessed by flow cytometry analysis and CCK-8 assay. In addition, the contents of malondialdehyde, reactive oxygen species, and superoxide dismutase were detected by corresponding commercial kits. The binding of miR-615-3p and MEF2A in human cardiomyocytes was examined by luciferase reporter assay.

Results: Hypoxia/reoxygenation treatment downregulated the expression level of miR-615-3p in human cardiomyocytes. Overexpressing miR-615-3p increased human cardiomyocyte viability and decreased human cardiomyocyte apoptosis. Moreover, miR-615-3p mimics suppressed oxidative stress in hypoxia/reoxygenation-stimulated human cardiomyocytes. MEF2A was confirmed as a target gene of miR-615-3p and was highly expressed in hypoxia/reoxygenation-stimulated human cardiomyocytes, and its upregulation partially reversed the influence of miR-615-3p mimics on oxidative stress and apoptosis of human cardiomyocytes. Moreover, miR-615-3p inactivated the P13K/Akt pathway by inhibiting MEF2A.

Conclusions: Overexpression of miR-615-3p protects human cardiomyocytes from oxidative stress injury by targeting MEF2A via the PI3K/Akt signaling.

Keywords: MiR-615-3p, MEF2A, oxidative stress, myocardial infarction

INTRODUCTION

Myocardial infarction (MI) is a typical coronary heart disease, which seriously endangers human health.[1,2] Although treatments for MI have been improved over the years, the mortality rate is still high.[3,4] Therefore, new treatments at the molecular level are urgently needed. Importantly, it has been suggested that the hypoxia/reoxygenation (H/R) injury and apoptosis of myocardial cells are the reasons for the occurrence of MI.[5,6] Various studies have reported that oxidative stress is also the main cause of MI.[7-11] H/R injury is associated with mitochondrial damage[12-16] and induces the increased reactive oxygen species (ROS) levels.[17] Thus, the inhibition of cell apoptosis and oxidative stress under myocardial H/R injury might serve as a key approach for treating MI.

MicroRNAs (miRs/miRNAs) are involved in a wide range of biological processes and can regulate gene expression by degrading or inhibiting the translation of target mRNAs.[18-20] The mature miRNA consists of approximately 22 nucleotides and regulates the target mRNA by specifically connecting to the 3′-untranslated region (3′-UTR) of the target mRNA.[21] In recent years, relevant studies have confirmed that miRNAs can affect the occurrence of cardiovascular diseases by regulating the functions of cardiac myocytes.[22,23] For example, miR-323-3p inhibits oxidative

Dongying Zhang
Gang Zhang
Kun Yu
Xiwen Zhang
Aixia Jiang

Department of Cardiology, The Affiliated Huaian No. 1 People's Hospital of Nanjing Medical University, Huaian, Jiangsu, China

Corresponding author:
Aixia Jiang
✉ hayyjax@njmu.edu.cn

Received: August 23, 2021
Accepted: December 6, 2021
Available Online Date: April 22, 2022

Cite this article as: Zhang D, Zhang G, Yu K, Zhang X, Jiang A. MiRNA-615-3p alleviates oxidative stress injury of human cardiomyocytes via PI3K/Akt signaling by targeting MEF2A. Anatol J Cardiol 2022;26(5):373-381.

DOI:10.5152/AnatolJCardiol.2021.901

stress and apoptosis of cardiomyocytes via regulation of the TGF-β2/JNK pathway.[24] Mir-124 targeting Dhcr24 regulates oxidative stress and cardiomyocyte apoptosis.[25] MiR-22 is also involved in the occurrence of MI.[26] It was also reported that miR-615-3p has an inhibitory effect on various diseases through diverse mechanisms.[27-29] Importantly, miR-615-3p has been reported as a downregulated miRNA in acute MI.[30] However, the corresponding mechanisms of miR-615-3p in oxidative stress injury of HCMs have not been studied yet.

Myocyte enhancer factor 2A (MEF2A) is a widely distributed DNA-binding transcription factor.[31] New evidence suggests that the MEF2 family interacts with multiple signaling pathways and is involved in the development of a variety of human diseases.[32-34] Moreover, MEF2A has been suggested to have an inhibitory effect on cell senescence by positively regulating the PI3K/Akt signaling pathway.[35] It has also been reported that PI3K and Akt activation is implicated in oxidative stress and apoptosis in MI.[36]

We hypothesized that miR-615-3p is involved in the H/R-stimulated injury of HCMs and its function is associated with the MEF2A/PI3K/Akt pathway. In this study, we focused on exploring the role of miR-615-3p on oxidative stress and apoptosis in H/R-stimulated human cardiomyocytes (HCMs) and explored its downstream pathway.

METHODS

Ethical Approval

Our study did not require an ethical board approval because it did not contain human or animal trials.

Cell Culture and Treatment

HCMs were purchased from Lonza (Walkersville, Maryland, United States) and were cultured in fibroblast growth medium (FGM) containing 500 mL of basal medium, 10 mL of fetal bovine serum, 5 mL of fibroblast growth supplement, and 5 mL of antibiotics at 37°C in a humid incubator with 5% CO_2 and 95% air. MiR-615-3p mimics (miR mimics), and the corresponding negative control (NC mimics) were purchased from RiboBio (Guangzhou, China). The MEF2A-overexpressing vector (pcDNA3.1-MEF2A), and the NC (empty pcDNA3.1) were synthesized by GenePharma (Shanghai, China). All the oligonucleotides and vectors were transfected into HCMs using the Lipofectamine 2000 reagent (Invitrogen, Carlsbad) at room temperature for 48 hours according to the manufacturer's instructions. HCMs in the control group were cultured under normal oxygen conditions. After transfection for 48 hours, cells received H/R treatment. Cells were incubated in serum-free DMEM in a hypoxia chamber (Biospherix, Lacona, NY, USA) for 30 minutes with 5% CO_2 and 95% N_2. The reoxygenation was conducted in a humidified atmosphere containing 5% CO_2 and 95% air at 37°C for 1 hour in DMEM/F12 containing 10% FBS. After 48 hours of reoxygenation, the cells were collected to detect gene expression, oxidative stress, and apoptosis.

HIGHLIGHTS

- Overexpression of miR-615-3p alleviates apoptosis and oxidative stress.
- MEF2A is a target gene of miR-615-3p.
- Overexpressed MEF2A reverses the inhibitory effects of miR-615-3p overexpression on oxidative stress and apoptosis.
- Mir-615-3p inactivates the P13K/Akt pathway by inhibiting MEF2A.

Reverse Transcription-Quantitative Polymerase Chain Reaction (RT-qPCR)

RNA samples from HCMs were extracted by TRIzol reagent (Takara Bro Inc, 9108). Hiscript ® III Reverse Transcriptase kit (cat. # R302-01; Vazyme) was used to synthesize cDNA from 1 μg of total RNA. SYBR-Green system (Toyobo Life Sciences) was used to perform qPCR with specific primers. GAPDH was an internal control. The primers are as follows: MEF2A, forward: 5′-CAC TCA ACC TCT TGC TAC C-3′, reverse: 5′-GTG AAT AAT CAG TGT TGT AGG C-3′; miR-615-3p, forward: 5′-ACA CTC CAG CTG GGT CCG AGC CTG GGT CTC-3′, reverse: 5′-TGG TGT CGT GGA GTC G-3′; GAPDH, forward: 5′-TCA AGA TCA TCA GCA ATG CC-3′, reverse: 5′-CGA TAC CAA AGT TGT CAT GGA-3′. The relative expression of the genes was calculated by the $2^{-\Delta\Delta Cq}$ method.[37]

Detection of Intracellular ROS Production

Intracellular ROS accumulation in HCMs was detected using a ROS assay kit (cat. # S0033S; Beyotime Institute of Biotechnology, Haimen, China). HCMs were cultured in a 96-well plate with 10 μmol/L of H2DCF-DA for 1 hour at 37°C. A fluorescence plate reader (BD Falcon, San Jose, CA, USA) was applied to evaluate the fluorescence intensity at Ex./Em. = 488/525 nm.

Detection of Malondialdehyde (MDA) Concentration and Sodium Superoxide (SOD) Enzymic Activity

After 48 hours of culture, HCMs of each group were collected and washed three times with PBS. After being centrifuged for 5 minutes at 1000 r/min, cell lysates were mixed with PBS and added to the incubator, which was cultured for 10 minutes at 4°C. Next, the supernatant was harvested after 5 minutes of centrifugation at 12 000 r/min to obtain the contents of MDA. MDA concentration was measured using an MDA Kit (cat. # S0131S; Beyotime Biotech, Shanghai, China). SOD enzymic activity was determined using a commercially available colorimetric assay kit (cat. # ab65354; Abcam, Cambridge, UK).

Detection of Cellular ATP Levels

The firefly luciferase-based ATP assay kit (cat. # S0027; Beyotime, Shanghai, China) was used to measure ATP production. Briefly, HCMs were lysed and centrifuged at 12 000× g. To conduct a subsequent reaction, the supernatant was then mixed with the ATP detection solution. Luminance was measured with a multifunctional microplate reader (BIO-TEK).

Flow Cytometry

The apoptosis rate of HCMs was detected by flow cytometry using Annexin V-FITC kit (cat. # C1062S; Beyotime). Next, the apoptotic cells were double stained with propidium iodide

(cat. # ST511; Beyotime) and Annexin V-fluorescein isothiocyanate. Finally, fluorescence was analyzed on a FACSCanto flow cytometer (Becton Dickinson, NJ, USA). FACSDiva 6.0 software was used for data analysis.

Western Blot Analysis

The proteins were separated from HCM cells with RIPA lysis buffer (cat. # P0013B; Beyotime). The protein concentration was evaluated by a BCA Protein Assay Kit (cat. # P0012S; Beyotime). The isolated protein was transferred into the PVDF membrane and blocked with 5% skim milk for 1 hour. The primary antibodies include anti-MEF2A (ab197070, 1 : 1000), anti-GAPDH (ab8245, 1 : 10 000), anti-PI3K (anti-PI3K, 1 : 1000), and anti-Akt (ab38449, 1 : 1000). The membranes were incubated with the horseradish peroxidase-conjugated secondary antibodies at 4°C overnight. The ECL chemiluminescence system was used to detect the immunoblots. Gray values of the protein bands were analyzed by the ImageJ software.

Luciferase Reporter Assay

HCMs were transfected with the plasmids that contain the wild-type MEF2A 3′-UTR, mutant MEF2A 3′-UTR, and miR-615-3p mimics or its negative control using Lipofectamine 2000. After 48 hours, luciferase activity was determined by normalizing firefly luciferase to renilla luciferase using a Dual-Luciferase Reporter Gene Assay Kit (cat. # RG027; Beyotime).

Cell Counting Kit-8 (CCK-8) Assay

First, HCMs (1×10^4 cells/well) were seeded into the 96-well plates. After incubation for 48 hours, CCK-8 solution (cat. # C0037; Beyotime) was added to test cell viability at 37°C. After HCMs being cultured for 24 hours, 48 hours, and 72 hours, cell viability was determined by measuring the absorbance at the wavelength of 450 nm using a microplate reader (Bio-Rad, Hercules, Calif, USA).

Statistical Analysis

Data are expressed as the mean ± standard deviation (SD) from three independent experiments. Each trial was repeated in triplicate. Detailed information has been provided in Supplementary Table 1. GraphPad Prism 7 (La Jolla, Calif, USA) and SPSS 19.0 (IBM, Armonk, NY, USA) were used to analyze the experimental results. Student's *t*-test was used to compare the differences between two groups, for example, gene expression in control cells and H/R-treated cells, or in cells transfected with NC mimics and miR-615-3p mimics. The normality test used in the study was Shapiro–Wilk (S–W) test. The one-way analysis of variance (ANOVA) followed by Tukey's post hoc test was adopted for difference comparison among more than 2 groups. The significance level was accepted as $P < .05$.

RESULTS

Overexpression of miR-615-3p Alleviates Apoptosis and Oxidative Stress

We first detected miR-615-3p expression by RT-qPCR, which showed that H/R treatment decreased the miR-615-3p expression (Figure 1A). The overexpression efficiency of miR-615-3p was examined, and we found that the expression level of miR-615-3p was significantly higher in the miR-615-3p mimics group than NC mimics group in HCMs (Figure 1B). CCK-8 was used to examine the cell viability of HCMs. MiR-615-3p overexpression rescued the H/R-induced suppressive effects on cell viability (Figure 1C). According to the flow cytometry analysis, H/R treatment increased the cell apoptosis rate of HCMs, while miR-615-3p mimics decreased it (Figure 1D and E). H/R induced the increased ROS levels in HCMs, and ROS levels in the miR-615-3p mimics group were lower than that in NC mimics group in H/R-stimulated HCMs (Figure 1F). Subsequently, ELISA was conducted to detect the changes in MDA and SOD in HCMs. H/R-induced the increase in MDA content and the decrease in SOD activity in HCMs were rescued by miR-615-3p mimics (Figure 1G and H). Finally, miR-615-3p mimics rescued the H/R-induced increase of ATP concentration in HCMs (Figure 1I). Collectively, these data indicated that miR-615-3p overexpression suppressed cell apoptosis and oxidative stress injury in H/R-stimulated HCMs.

MEF2A is a Target Gene of miR-615-3p

The miRDB database (http://mirdb.org/) shows that a total of 36 mRNAs contain binding sites on miR-615-3p. The expression levels of the six target genes (PSMD11, ZNF626, ITSN1, MEF2A, USP44, and TOMM7) in HCMs after H/R were examined (Figure 2A). Among all the target genes, the MEF2A expression was significantly promoted in H/R-stimulated HCMs. Similarly, the protein level of MEF2A was also increased in H/R-stimulated HCMs according to the results of western blot (Figure 2B). Furthermore, the binding site between miR-615-3p and MEF2A was predicted by the Targetscan website. These binding sites were highly-conservated among different species (human, chimp, rhesus, squirrel, mouse, etc.) (Figure 2C). The construct of the pmiR-RB-Report-MEF2A -3'UTR-WT/MUT vector was shown in Figure 2D. Next, the luciferase reporter assay further confirmed the interaction between miR-615-3p and MEF2A 3′-UTR. MiR-615-3p significantly reduced the luciferase activity of plasmids containing wild-type MEF2A 3′-UTR, while that of mutant MEF2A 3′-UTR remained almost unchanged (Figure 2E). In line with the results of the luciferase reporter assay, we found that miR-615-3p overexpression downregulated the mRNA expression and protein levels of MEF2A in HCMs (Figure 2F and G). Collectively, miR-615-3p was a MEF2A-targeting miRNA that negatively modulates its expression.

Overexpressed MEF2A Reverses the Inhibitory Effects of miR-615-3p Overexpression on Oxidative Stress and Apoptosis

According to the results of RT-qPCR and western blot, miR-615-3p mimics inhibited the expression of MEF2A, which was then promoted by pcDNA3.1-MEF2A (Figure 3A and B). CCK-8 assay showed a reduction of cell viability in the miR-615-3p+MEF2A group, compared with the miR-615-3p mimics group (Figure 3C). MEF2A overexpression also increased the apoptosis rate of HCMs, compared with the miR-615-3p mimics group, as revealed by flow cytometry analysis (Figure 3D and E). MEF2A overexpression rescued the suppressive effect of miR-615-3p mimics on ROS accumulation (Figure 3F). Similarly, according to ELISA, miR-615-3p overexpression

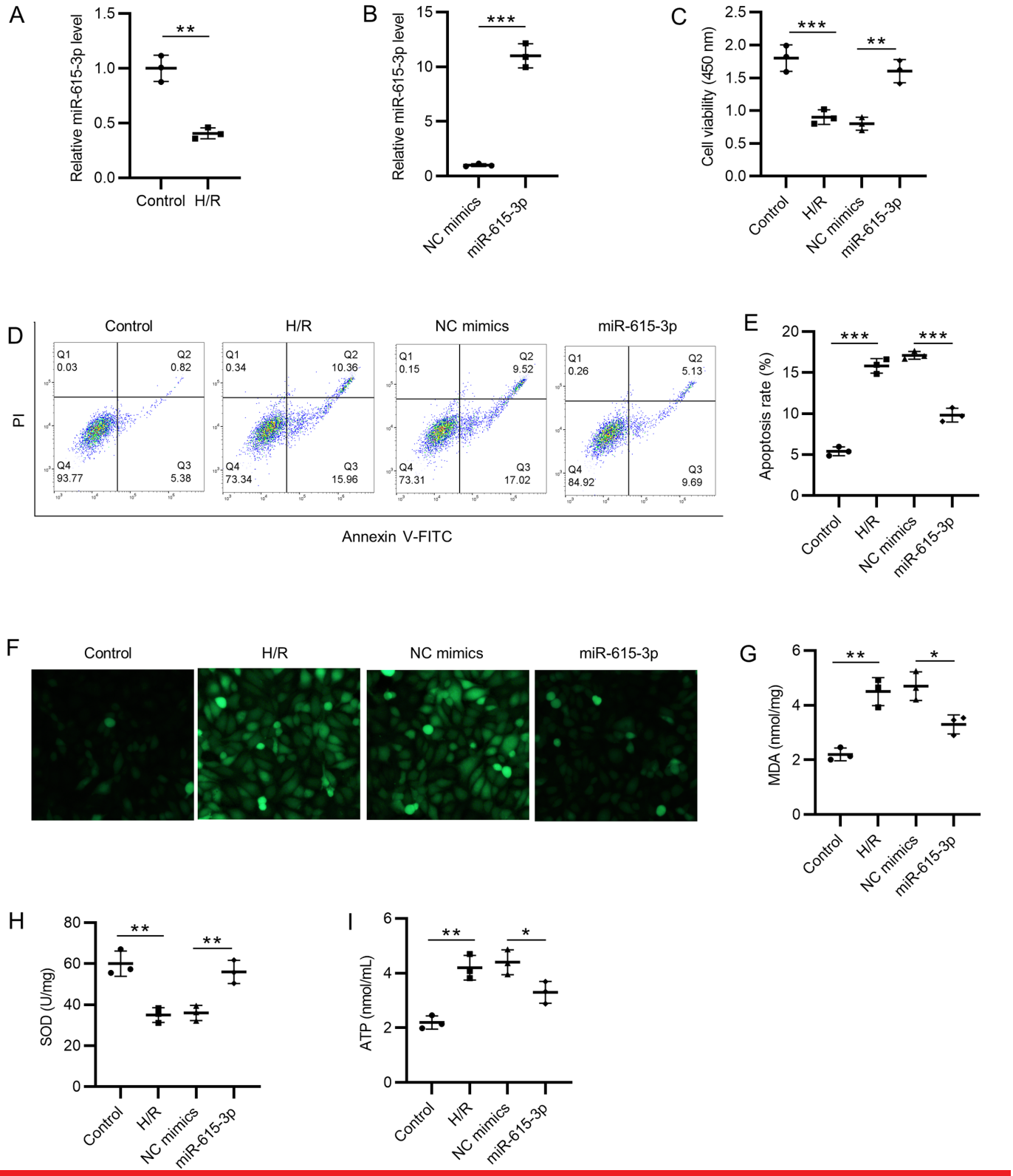

Figure 1. Overexpression of miR-615-3p alleviates apoptosis and oxidative stress. (A) The expression level of miR-615-3p in H/R-stimulated HCMs was examined by RT-qPCR. (B) Overexpression efficiency of miR-615-3p was detected by RT-qPCR. (C) Cell viability of HCMs in control, H/R, H/R+NC mimics, and H/R+miR-615-3p mimics group was confirmed by CCK-8. (D-E) Cell apoptosis rates of HCMs in different groups were detected by flow cytometry. (F) ROS levels in HCMs in different groups. (G-H) The changes in MDA concentration and SOD enzymic activity in HCMs were detected by corresponding commercial kits. (I) ATP levels in HCMs in different groups were measured. *$P < .05$, **$P < .01$, ***$P < .001$. HCMs, human cardiomyocytes; RT-qPCR, reverse transcription-quantitative polymerase chain reaction; ROS, reactive oxygen species.

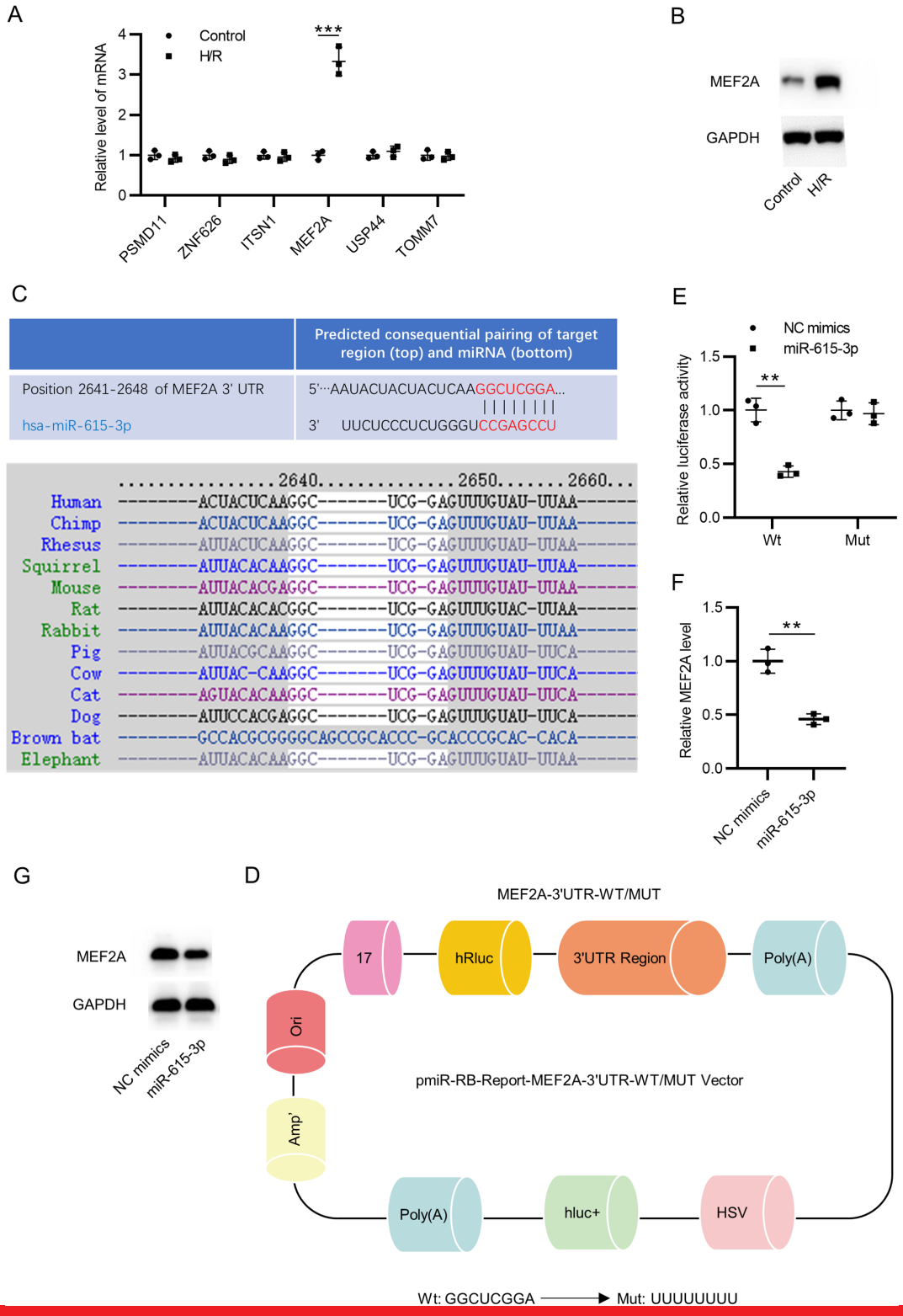

Figure 2. MEF2A is a target gene of miR-615-3p. (A) The expression levels of the six target genes (PSMD11, ZNF626, ITSN1, MEF2A, USP44, and TOMM7) in HCMs were examined by RT-qPCR. (B) Western blot was conducted to examine the protein level of MEF2A in H/R-stimulated HCMs. (C) Targetscan predicted the binding sites between miR-615-3p and MEF2A 3'-UTR. (D) Schematic diagram of the pmiR-RB-Report-MEF2A-3'UTR-WT/MUT vector. (E) Luciferase activities of HCMs transfected with luciferase reporter vectors and miR-615-3p mimics were assessed. (F-G) The mRNA expression and protein levels of MEF2A in HCMs transfected with miR-615-3p mimics were detected by RT-qPCR and western blot, respectively; **$P < .01$, ***$P < .001$. HCMs, human cardiomyocytes; RT-qPCR, reverse transcription-quantitative polymerase chain reaction; H/R, hypoxia/reoxygenation; UTR, untranslated region.

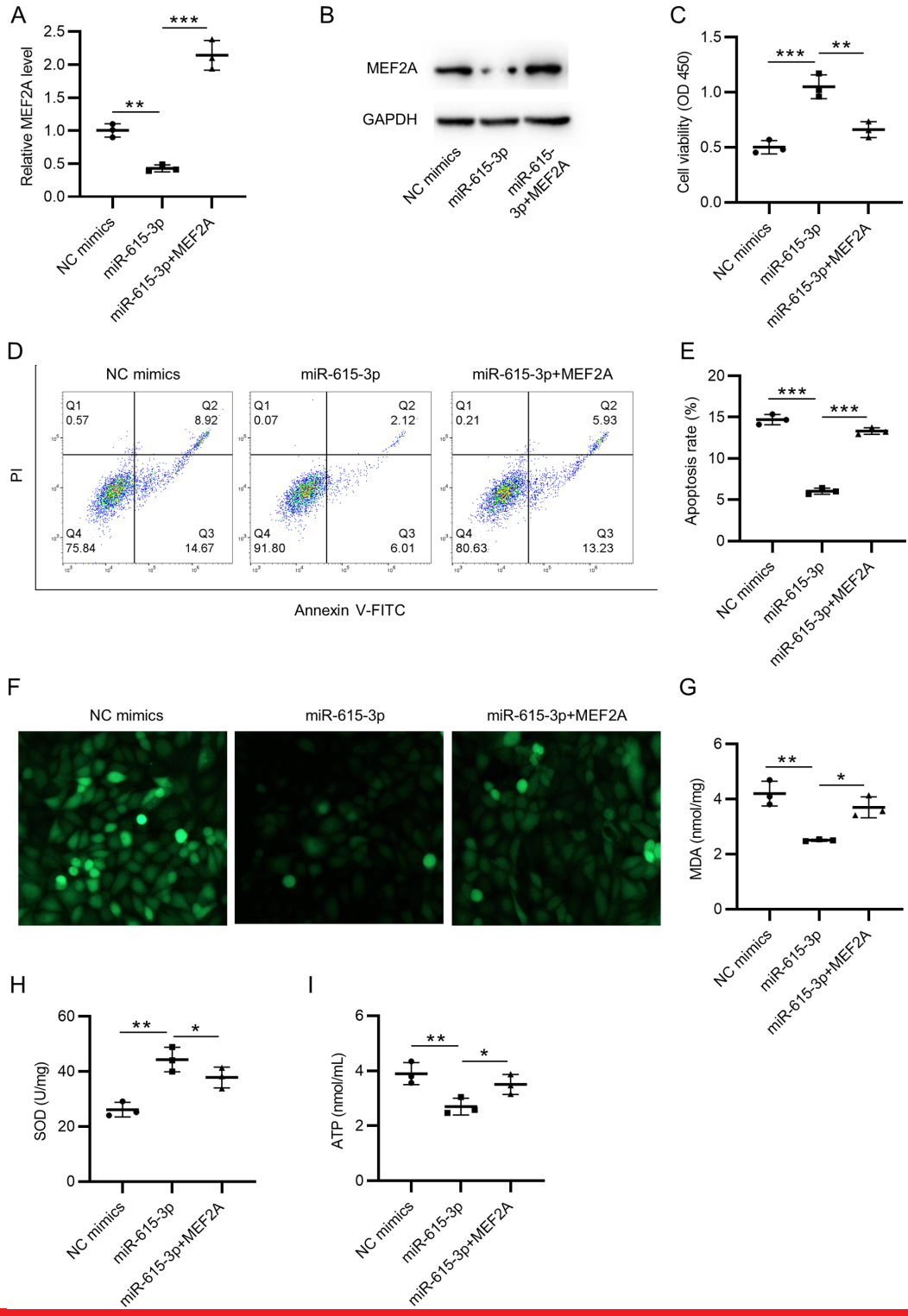

Figure 3. Overexpressed MEF2A reverses the inhibitory effects of miR-615-3p overexpression on oxidative stress and apoptosis. (A-B) The mRNA expression and protein levels of MEF2A in HCMs transfected with NC mimics, miR-615-3p mimics, or cotransfected with miR-615-3p mimics+pcDNA3.1-MEF2A were examined by RT-qPCR and Western blot, respectively. (C) CCK-8 assay showed the cell viability of HCMs in three groups. (D-E) Flow cytometry was conducted to examine the apoptosis rates of HCMs transfected with NC mimics, miR-615-3p mimics, or cotransfected with miR-615-3p mimics+pcDNA3.1/MEF2A. (F) H2DCF-DA staining was used to detect ROS accumulation. (G-H) The rescue effects of MEF2A on miR-615-3p in MDA concentration and SOD enzymic activity were measured. (I) The rescue effect of MEF2A overexpression on miR-615-3p in ATP level was measured. *$P < .05$, **$P < .01$, ***$P < .001$. HCMs, human cardiomyocytes; RT-qPCR, reverse transcription-quantitative polymerase chain reaction; ROS, reactive oxygen species.

suppressed the intracellular MDA content and promoted SOD activities, while these effects were further reversed by excessive MEF2A (Figure 3G and H). Finally, miR-615-3p mimics reduced ATP production, while MEF2A overexpression reversed it and promoted ATP production (Figure 3I). All these results indicated that overexpressed MEF2A partially counteracted the inhibitory effects of miR-615-3p overexpression on oxidative stress and apoptosis in HCMs.

Mir-615-3p Inactivates the P13K/Akt Pathway by Inhibiting MEF2A

Levels of phosphorylated PI3K and Akt proteins were enhanced after H/R treatment as compared with the control group. Overexpressed miR-615-3p significantly decreased phosphorylation of PI3K and Akt proteins in HCMs, while overexpressed MEF2A partially rescued the reduction. Thus, miR-615-3p inactivated the P13K/Akt pathway by inhibiting the expression level of MEF2A (Figure 4A and B).

DISCUSSION

Cardiomyocyte is essential for blood supply and oxygen supply and its damage and death contribute to the pathogenesis of MI.[38] Notably, the reduction of oxidative stress and apoptosis in HCMs contributes to the development of MI.[39] Currently, emerging studies have confirmed the importance of miRNAs in the pathology and physiology of cardiovascular diseases, for example, it has been shown that miR-21, miR-133, and miR-499 can prevent the oxidative stress and apoptosis of cardiomyocytes, while miR-1, miR199a, and miR-320 can facilitate oxidative stress and apoptosis.[40] Although miR-651-3p has been reported to be lowly expressed in AMI,[30] the detailed biological function of miR-651-3p in MI remains unknown. In this study, we investigated the expression of miR-615-3p in H/R-stimulated HCMs and confirmed its downregulation, which is in consistent with the previous study at the *in vitro* level. Moreover, we figured out the biological role of miR-615-3p in HCMs and revealed its inhibitory effect on oxidative stress and apoptosis in HCMs. To explore the concrete mechanism of miR-651-3p, we further analyzed its downstream target genes and relevant signaling pathways.

The effect of MEF2A on cardiac myocyte function has been reported in previous studies. For example, the Akt2 deficiency mediated downregulation of MEF2A impairs hypertrophy in cardiomyocytes.[33] MEF2A induces cardiomyocyte hypertrophy through an EGFR-ERK5-HB-EGF-COX-2 pathway.[41] MEF2 is associated with cardiomyocyte apoptosis and hypertrophy.[42] In our study, MEF2A was significantly upregulated in H/R-stimulated HCMs, indicating the close association of MEF2A and the H/R-stimulated injury of HCMs, which led us to focus on MEF2A for further investigation. Next, we found that miR-615-3p mimics significantly decreased the mRNA expression and protein levels of MEF2A, which suggested the negative regulation of miR-615-3p on MEF2A. Subsequently, MEF2A reversed the inhibitory effect of miR-615-3p overexpression on oxidative stress and apoptosis of H/R-treated HCMs. These findings indicated that miR-615-3p regulates the oxidative stress and apoptosis of H/R-treated HCMs by MEF2A, indicating the potential miR-615-3p/MEF2A axis in MI. However, the concrete mechanism of MEF2A needed further investigation, and we subsequently explored the potential signaling pathways that are regulated by the miR-651-3p/MEF2A axis.

In a previous study, PI3K/Akt signaling has been shown to be directly regulated by MEF2A.[35] Importantly, another study has demonstrated that oxidative stress was inhibited by PI3K/Akt inhibitor in rats with diabetic cardiomyopathy.[43] The PI3K/Akt pathway plays a protective role in cardiomyocytes against the H/R-induced oxidative stress and apoptosis.[44,45] Thus, we hypothesized that the miR-615-3p/MEF2A axis might affect oxidative stress and apoptosis via the PI3K/Akt pathway in HCMs. Western blot was used to verify our hypothesis. We found that overexpressed

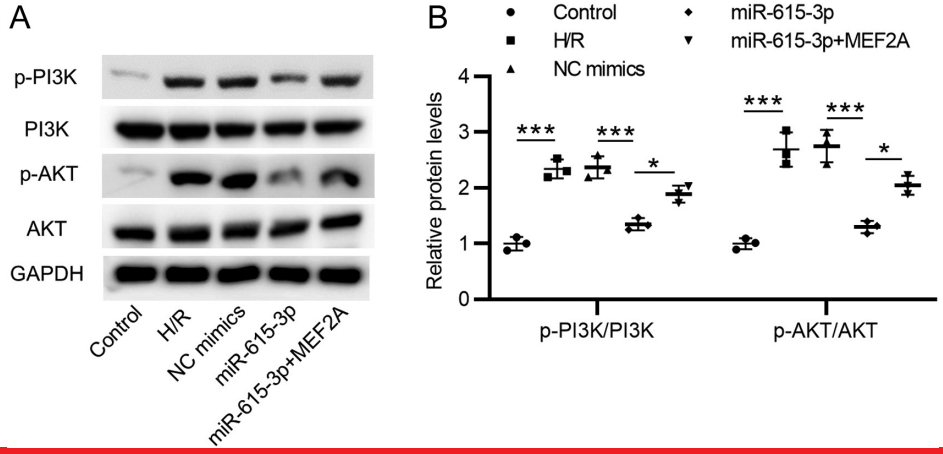

Figure 4. Mir-615-3p inactivates the P13K/Akt pathway by inhibiting MEF2A. (A-B) H/R-stimulated HCMs were pretreated with NC mimics, miR-615-3p mimics, or cotreated with miR-615-3p mimics+MEF2A overexpression vector, and the protein levels of phosphorylated PI3K, Akt and total PI3K, Akt proteins were measured by Western blot analyses. *$P < .01$, ***$P < .001$. HCMs, human cardiomyocytes

miR-615-3p significantly decreased the phosphorylation of PI3K and Akt in HCMs, while overexpressed MEF2A partially rescued the reduction, suggesting that miR-615-3p suppresses the PI3K/Akt pathway in HCMs by MEF2A. In other words, the rescue effects of miR-615-3p on the H/R-induced oxidative stress and apoptosis of HCMs were achieved by the MEF2A/PI3K/Akt pathway. Another study also reveals that miR-615-3p inactivates the PI3K/Akt pathway.[46] However, in contradiction with our study, a previous study revealed the positive association of miR-615-3p and the PI3K/Akt pathway.[47] Moreover, our results lack the support of *in vivo* experiments. In addition, whether other target genes (PSMD11, ZNF626, ITSN1, USP44, and TOMM7) play the same role as MEF2A in H/R-stimulated HCMs is unknown, and the specific mechanism of H/R-induced abnormal expression of miR-615-3p needed to be clarified in subsequent studies.

To conclude, miR-615-3p exhibited a decreased expression level in H/R-stimulated HCMs and miR-615-3p mimics alleviated the oxidative stress and apoptosis. Functionally, as a target gene of miR-615-3p, MEF2A overexpression reversed the inhibitory effect of miR-615-3p on oxidative stress and apoptosis in HCMs. We further confirmed that miR-615-3p attenuated oxidative stress injury of HCMs by inactivating the PI3K/Akt signaling pathway by inhibiting MEF2A. Our results indicated that miR-615-3p/MEF2A axis may provide novel research strategies and biomarkers for MI.

Ethics Committee Approval: Our study did not require an ethical board approval because it did not contain human or animal trials.

Peer-review: Externally peer-reviewed.

Author Contributions: Concept – D.Z., A.J.; Design – D.Z., G.Z., A.J.; Supervision – D.Z., A.J.; Fundings – None; Materials – D.Z., G.Z., K.Y., A.J.; Data Collection and/or Processing – G.Z., X.Z.; Analysis and/or Interpretation – D.Z., X.Z., A.J.; Literature Review – D.Z., K.Y.; Writing – D.Z.; Critical Review – A.J.

Declaration of Interests: The authors declared no competing interests in this study.

Funding: This research received no specific grant from any funding agency in the public, commercial, or not-for-profit sectors.

REFERENCES

1. Benjamin EJ, Virani SS, Callaway CW, et al. Heart disease and stroke Statistics-2018 update: a report From the American Heart Association. *Circulation*. 2018;137(12):e67-e492. [CrossRef]
2. Qiu H, Liu JY, Wei D, et al. Cardiac-generated prostanoids mediate cardiac myocyte apoptosis after myocardial ischaemia. *Cardiovasc Res*. 2012;95(3):336-345. [CrossRef]
3. Khairy P, Thibault B, Talajic M, et al. Prognostic significance of ventricular arrhythmias post-myocardial infarction. *Can J Cardiol*. 2003;19(12):1393-1404.
4. Davidson SM, Ferdinandy P, Andreadou I, et al. Multitarget strategies to reduce myocardial ischemia/reperfusion injury: JACC review topic of the week. *J Am Coll Cardiol*. 2019;73(1):89-99. [CrossRef].
5. Katz AM, Messineo FC. Lipid-membrane interactions and the pathogenesis of ischemic damage in the myocardium. *Circ Res*. 1981;48(1):1-16. [CrossRef]
6. Abbate A, Narula J. Role of apoptosis in adverse ventricular remodeling. *Heart Fail Clin*. 2012;8(1):79-86. [CrossRef]
7. Navarro-Yepes J, Burns M, Anandhan A, et al. Oxidative stress, redox signaling, and autophagy: cell death versus survival. *Antioxid Redox Signal*. 2014;21(1):66-85. [CrossRef]
8. Zhao ZQ. Oxidative stress-elicited myocardial apoptosis during reperfusion. *Curr Opin Pharmacol*. 2004;4(2):159-165. [CrossRef]
9. Hertog MG, Feskens EJ, Hollman PC, Katan MB, Kromhout D. Dietary antioxidant flavonoids and risk of coronary heart disease: the Zutphen Elderly Study. *Lancet*. 1993;342(8878):1007-1011. [CrossRef]
10. Ye Y, Li J, Yuan Z. Effect of antioxidant vitamin supplementation on cardiovascular outcomes: a meta-analysis of randomized controlled trials. *PLoS One*. 2013;8(2):e56803. [CrossRef]
11. Asplund K. Antioxidant vitamins in the prevention of cardiovascular disease: a systematic review. *J Intern Med*. 2002;251(5):372-392. [CrossRef]
12. Wang J, Zhou H. Mitochondrial quality control mechanisms as molecular targets in cardiac ischemia-reperfusion injury. *Acta pharm Sin B*. 2020;10(10):1866-1879. [CrossRef]
13. Wang J, Toan S, Zhou H. Mitochondrial quality control in cardiac microvascular ischemia-reperfusion injury: new insights into the mechanisms and therapeutic potentials. *Pharmacol Res*. 2020;156:104771. [CrossRef]
14. Zhou H, Toan S, Zhu P, Wang J, Ren J, Zhang Y. DNA-PKcs promotes cardiac ischemia reperfusion injury through mitigating BI-1-governed mitochondrial homeostasis. *Basic Res Cardiol*. 2020;115(2):11. [CrossRef]
15. Wang J, Zhu P, Li R, Ren J, Zhou H. Fundc1-dependent mitophagy is obligatory to ischemic preconditioning-conferred renoprotection in ischemic AKI via suppression of Drp1-mediated mitochondrial fission. *Redox Biol*. 2020;30:101415. [CrossRef]
16. Zhou H, Zhu P, Wang J, Toan S, Ren J. DNA-PKcs promotes alcohol-related liver disease by activating Drp1-related mitochondrial fission and repressing FUNDC1-required mitophagy. *Signal Transduct Target Ther*. 2019;4:56. [CrossRef]
17. Wang J, Toan S, Zhou H. New insights into the role of mitochondria in cardiac microvascular ischemia/reperfusion injury. *Angiogenesis*. 2020;23(3):299-314. [CrossRef]
18. Krol J, Loedige I, Filipowicz W. The widespread regulation of microRNA biogenesis, function and decay. *Nat Rev Genet*. 2010;11(9):597-610. [CrossRef]
19. Guo H, Ingolia NT, Weissman JS, Bartel DP. Mammalian microRNAs predominantly act to decrease target mRNA levels. *Nature*. 2010;466(7308):835-840. [CrossRef]
20. Baek D, Villén J, Shin C, Camargo FD, Gygi SP, Bartel DP. The impact of microRNAs on protein output. *Nature*. 2008;455(7209):64-71. [CrossRef]
21. Pal AS, Kasinski AL. Animal models to study microRNA function. *Adv Cancer Res*. 2017;135:53-118. [CrossRef]
22. Condorelli G, Latronico MV, Dorn GW, 2nd. microRNAs in heart disease: putative novel therapeutic targets? *Eur Heart J*. 2010;31(6):649-658. [CrossRef]
23. Schulte C, Zeller T. microRNA-based diagnostics and therapy in cardiovascular disease-Summing up the facts. *Cardiovasc Diagn Ther*. 2015;5(1):17-36. [CrossRef]
24. Shi CC, Pan LY, Zhao YQ, Li Q, Li JG. MicroRNA-323-3p inhibits oxidative stress and apoptosis after myocardial infarction by targeting TGF-β2/JNK pathway. *Eur Rev Med Pharmacol Sci*. 2020;24(12):6961-6970. [CrossRef]

25. Han F, Chen Q, Su J, et al. MicroRNA-124 regulates cardiomyocyte apoptosis and myocardial infarction through targeting Dhcr24. *J Mol Cell Cardiol*. 2019;132:178-188. [CrossRef]
26. Cong BH, Zhu XY, Ni X. The roles of microRNA-22 in myocardial infarction. *Sheng Li Xue bao: Acta physiologica Sinica*. 2017;69(5):571-578.
27. Yin J, Zhuang G, Zhu Y, et al. MiR-615-3p inhibits the osteogenic differentiation of human lumbar ligamentum flavum cells via suppression of osteogenic regulators GDF5 and FOXO1. *Cell Biol Int*. 2017;41(7):779-786. [CrossRef]
28. Liu J, Jia Y, Jia L, Li T, Yang L, Zhang G. *MicroRNA*. 615-3p Inhibits the Tumor Growth and Metastasis of NSCLC via Inhibiting IGF2. *Oncol Res*. 2019;27(2):269-279. [CrossRef]
29. Pu HY, Xu R, Zhang MY, et al. Identification of microRNA-615-3p as a novel tumor suppressor in non-small cell lung cancer. *Oncol Lett*. 2017;13(4):2403-2410. [CrossRef]
30. Zhong Z, Wu H, Zhong W, Zhang Q, Yu Z. Expression profiling and bioinformatics analysis of circulating microRNAs in patients with acute myocardial infarction. *J Clin Lab Anal*. 2020;34(3):e23099. [CrossRef]
31. McKinsey TA, Zhang CL, Olson EN. MEF2: a calcium-dependent regulator of cell division, differentiation and death. *Trends Biochem Sci*. 2002;27(1):40-47. [CrossRef]
32. Naya FJ, Black BL, Wu H, et al. Mitochondrial deficiency and cardiac sudden death in mice lacking the MEF2A transcription factor. *Nat Med*. 2002;8(11):1303-1309. [CrossRef]
33. Chen D, Chen F, Xu Y, et al. AKT2 deficiency induces retardation of myocyte development through EndoG-MEF2A signaling in mouse heart. *Biochem Biophys Res Commun*. 2017;493(4):1410-1417. [CrossRef]
34. Chen X, Gao B, Ponnusamy M, Lin Z, Liu J. MEF2 signaling and human diseases. *Oncotarget*. 2017;8(67):112152-112165. [CrossRef]
35. Liu B, Wang L, Jiang W, et al. Myocyte enhancer factor 2A delays vascular endothelial cell senescence by activating the PI3K/p-Akt/SIRT1 pathway. *Aging*. 2019;11(11):3768-3784. [CrossRef]
36. Jiang T, Zhang L, Ding M, Li M. Protective effect of vasicine Against myocardial infarction in rats via modulation of oxidative stress, inflammation, and the PI3K/Akt pathway. *Drug Des Dev Ther*. 2019;13:3773-3784. [CrossRef]
37. Livak KJ, Schmittgen TD. Analysis of relative gene expression data using real-time quantitative PCR and the 2(-Delta Delta C(T)) Method. *Methods (San Diego Calif)*. 2001;25(4):402-408. [CrossRef]
38. Nabel EG, Braunwald E. A tale of coronary artery disease and myocardial infarction. *N Engl J Med*. 2012;366(1):54-63. [CrossRef]
39. Neri M, Fineschi V, Di Paolo M, et al. Cardiac oxidative stress and inflammatory cytokines response after myocardial infarction. *Curr Vasc Pharmacol*. 2015;13(1):26-36. [CrossRef]
40. Zhu H, Fan GC. Role of microRNAs in the reperfused myocardium towards post-infarct remodelling. *Cardiovasc Res*. 2012;94(2):284-292. [CrossRef]
41. Lee KS, Park JH, Lim HJ, Park HY. HB-EGF induces cardiomyocyte hypertrophy via an ERK5-MEF2A-COX2 signaling pathway. *Cell Signal*. 2011;23(7):1100-1109. [CrossRef]
42. Tobin SW, Hashemi S, Dadson K, et al. Heart failure and MEF2 transcriptome dynamics in response to β-blockers. *Sci Rep*. 2017;7(1):4476. [CrossRef]
43. Ma L, Li XP, Ji HS, Liu YF, Li EZ. Baicalein protects rats with diabetic cardiomyopathy Against oxidative stress and inflammation injury via phosphatidylinositol 3-kinase (PI3K)/AKT pathway. *Med Sci Monit*. 2018;24:5368-5375. [CrossRef]
44. Zhao S, Zhang C, Pi Z, Li R, Han P, Guo L. Oxycodone protects cardiomyocytes from ischemia-reperfusion-induced apoptosis via PI3K/Akt pathway. *Pharmazie*. 2020;75(9):430-435. [CrossRef]
45. Xin G, Xu-Yong L, Shan H, et al. SH2B1 protects cardiomyocytes from ischemia/reperfusion injury via the activation of the PI3K/AKT pathway. *Int Immunopharmacol*. 2020;83:105910. [CrossRef]
46. Sun L, Wang P, Zhang Z, et al. MicroRNA-615 functions as a tumor suppressor in osteosarcoma through the suppression of HK2. *Oncol Lett*. 2020;20(5):226. [CrossRef]
47. Feng H, Gui Q, Wu G, et al. Long noncoding RNA Nespas inhibits apoptosis of epileptiform hippocampal neurons by inhibiting the PI3K/Akt/mTOR pathway. *Exp Cell Res*. 2021;398(1):112384. [CrossRef]

Supplementary Table 1. Statistical Analysis of Experimental Results

		Figure 1A Experimental Results			
	n (Trials/Sample Size)	r (Replication Size)	Mean	Standard Deviation	*P*
Control	1	3	1.00	0.12	.001
H/R	1	3	0.41	0.05	

		Figure 1B Experimental Results			
	n (Trials/Sample Size)	r (Replication Size)	Mean	Standard Deviation	*P*
NC mimics	1	3	1.00	0.13	<0
miR-615-3p	1	3	11.00	1.10	

		Figure 1C Experimental Results			
	n (Trials/Sample Size)	r (Replication Size)	Mean	Standard Deviation	*P*
Control	1	3	1.80	0.20	< 0
H/R	1	3	0.90	0.11	
NC mimics	1	3	0.80	0.10	.001
miR-615-3p	1	3	1.60	0.18	

		Figure 1E Experimental Results			
	n (Trials/Sample Size)	r (Replication Size)	Mean	Standard Deviation	*P*
Control	1	3	5.41	0.55	< 0
H/R	1	3	15.81	0.89	
NC mimics	1	3	17.11	0.48	< 0
miR-615-3p	1	3	9.82	0.85	

		Figure 1G Experimental Results			
	n (Trials/Sample Size)	r (Replication Size)	Mean	Standard Deviation	*P*
Control	1	3	2.20	0.23	.001
H/R	1	3	4.50	0.51	
NC mimics	1	3	4.70	0.52	.015
miR-615-3p	1	3	3.30	0.35	

		Figure 1H Experimental Results			
	n (Trials/Sample Size)	r (Replication Size)	Mean	Standard Deviation	*P*
Control	1	3	60.00	6.20	.001
H/R	1	3	35.00	3.62	
NC mimics	1	3	36.00	3.70	.005
miR-615-3p	1	3	56.00	5.66	

		Figure 1I Experimental Results			
	n (Trials/Sample Size)	r (Replication Size)	Mean	Standard Deviation	*P*
Control	1	3	2.20	0.24	.001
H/R	1	3	4.20	0.45	
NC mimics	1	3	4.40	0.46	.038
miR-615-3p	1	3	3.30	0.40	

		Figure 2A Experimental Results			
PSMD11	n (Trials/Sample Size)	r (Replication Size)	Mean	Standard Deviation	*P*
Control	1	3	1.00	0.11	.372
H/R	1	3	0.92	0.09	

(*Continued*)

Supplementary Table 1. Statistical Analysis of Experimental Results (*Continued*)

ZNF626	n (Trials/Sample Size)	r (Replication Size)	Mean	Standard Deviation	*P*
Control	1	3	1.00	0.10	.294
H/R	1	3	0.90	0.10	
ITSN1	n (Trials/Sample Size)	r (Replication Size)	Mean	Standard Deviation	*P*
Control	1	3	1.00	0.09	.681
H/R	1	3	0.96	0.11	
MEF2A	n (Trials/Sample Size)	r (Replication Size)	Mean	Standard Deviation	*P*
Control	1	3	1.00	0.11	< 0
H/R	1	3	3.33	0.35	
USP44	n (Trials/Sample Size)	r (Replication Size)	Mean	Standard Deviation	*P*
Control	1	3	1.00	0.09	.336
H/R	1	3	1.10	0.13	
TOMM7	n (Trials/Sample Size)	r (Replication Size)	Mean	Standard Deviation	*P*
Control	1	3	1.00	0.12	.839
H/R	1	3	0.98	0.10	
		Figure 2E Experimental Results			
Wt	n (Trials/Sample Size)	r (Replication Size)	Mean	Standard Deviation	*P*
NC mimics	1	3	1.00	0.11	.001
miR-615-3p	1	3	0.43	0.05	
Mut	n (Trials/Sample Size)	r (Replication Size)	Mean	Standard Deviation	*P*
NC mimics	1	3	1.00	0.09	.72
miR-615-3p	1	3	0.97	0.10	
		Figure 2F Experimental Results			
	n (Trials/Sample Size)	r (Replication Size)	Mean	Standard Deviation	*P*
NC mimics	1	3	1.00	0.11	.002
miR-615-3p	1	3	0.46	0.05	
		Figure 3A Experimental Results			
	n (Trials/Sample Size)	r (Replication Size)	Mean	Standard Deviation	*P*
NC mimics	1	3	1.00	0.10	
miR-615-3p	1	3	0.43	0.05	.007
miR-615-3p+MEF2A	1	3	2.14	0.22	< 0
		Figure 3C Experimental Results			
	n (Trials/Sample Size)	r (Replication Size)	Mean	Standard Deviation	*P*
NC mimics	1	3	0.50	0.06	
miR-615-3p	1	3	1.05	0.11	< 0
miR-615-3p+MEF2A	1	3	0.66	0.07	.003
		Figure 3E Experimental Results			
	n (Trials/Sample Size)	r (Replication Size)	Mean	Standard Deviation	*P*
NC mimics	1	3	14.71	0.62	
miR-615-3p	1	3	6.04	0.37	< 0
miR-615-3p+MEF2A	1	3	13.31	0.40	< 0

(*Continued*)

Supplementary Table 1. Statistical Analysis of Experimental Results (*Continued*)

		Figure 3G Experimental Results			
	n (Trials/Sample Size)	r (Replication Size)	Mean	Standard Deviation	*P*
NC mimics	1	3	4.20	0.45	
miR-615-3p	1	3	2.50	0.03	.002
miR-615-3p+MEF2A	1	3	3.70	0.38	.012

		Figure 3H Experimental Results			
	n (Trials/Sample Size)	r (Replication Size)	Mean	Standard Deviation	*P*
NC mimics	1	3	26.10	2.65	
miR-615-3p	1	3	44.30	4.45	.002
miR-615-3p+MEF2A	1	3	31.00	3.89	.011

		Figure 3I Experimental Results			
	n (Trials/Sample Size)	r (Replication Size)	Mean	Standard Deviation	*P*
NC mimics	1	3	3.90	0.40	
miR-615-3p	1	3	2.20	0.34	.003
miR-615-3p+MEF2A	1	3	3.50	0.36	.012

		Figure 4A Experimental Results			
p-PI3K/PI3K	n (Trials/Sample Size)	r (Replication Size)	Mean	Standard Deviation	*P*
Control	1	3	1.00	0.12	
H/R	1	3	2.34	0.17	< 0
NC mimics	1	3	2.37	0.20	
miR-615-3p	1	3	1.35	0.11	0
miR-615-3p+MEF2A	1	3	1.89	0.15	.01
p-Akt/Akt	n (Trials/Sample Size)	r (Replication Size)	Mean	Standard Deviation	*P*
Control	1	3	1	0.1	
H/R	1	3	2.69	0.31	< 0
NC mimics	1	3	2.75	0.29	
miR-615-3p	1	3	1.30	0.11	0
miR-615-3p+MEF2A	1	3	2.05	0.17	.011